Annals of Mathematics and Computer Science ISSN: 2789-7206
Vol 37 (2026) 1-22 https://doi.org/10.56947/amcs.v37.960

WEIGHTED GAMMA-WEIBULL DISTRIBUTION FOR CLIMATE EXTREMES

FRED NYAMITAGO MONARI[1] AND EVALYNE KAGENDO RWITO[1]

Abstract. We propose a length-biased Weighted Gamma-Weibull Distribution (WGWD) for modeling extreme climate events. The size-biased weighting scheme enhances flexibility to capture bathtub-shaped hazard rates typical of climate extremes. We derive statistical properties including moment structures, hazard behavior, stochastic ordering, and information measures. Maximum likelihood estimation is developed with a custom iterative algorithm analyzed for convergence and computational complexity, and parameter identifiability is studied via the Fisher information matrix. Simulation studies validate estimator consistency, and application to a real-world climate dataset demonstrates superior performance over conventional distributions. The model provides a powerful tool for climate risk assessment under increasing extreme weather occurrences.

Keywords. Weighted distributions, gamma-Weibull distribution, extreme climate events, maximum likelihood estimation, hazard rate analysis, climate change modeling
2020 Mathematics Subject Classification. Primary 62E15; Secondary 62F10, 62P12

1. Introduction

Extreme events such as extreme climate events have become frequent and more intense over the past decades, becoming a serious challenge to statistical modeling in climate science [1]. Although they are fundamental to climate statistics, traditional probability distributions can be difficult to use because they tend to fail to portray the intricate patterns of extreme weather events such as heatwaves, lengthy droughts and heavy rainfall events [2]. The weaknesses of the traditional models have prompted continued analysis of more adaptable distributions capable of appropriately capturing the heavy-tailed, highly skewed as well as multimodal nature of climate extremes [3].

Weighted distributions provide a potential methodological approach to deal with these issues. The weighted distributions are originally proposed by [4] and modeled formally by [5] as ways of correcting selection biases and observational

Date: Received: Sep 6, 2026; Revised: Oct 2, 2026; Accepted: Oct 11, 2026.
* Corresponding author
© The Author(s) 2026. This article is licensed under a Creative Commons Attribution-NonCommercial-NoDerivatives 4.0 International License. To view a copy of the licence, visit https://creativecommons.org/licenses/by-nc-nd/4.0/.

restrictions by modifying the probability models of the baseline by using weight functions that are non-negative and integrable to a factor. It is specifically applicable in climate science, where measurement devices and networks of observation might inefficiently capture or overcapture some classes of events systematically [6].

The Gamma-Weibull distribution which was presented in the gamma-X family generator by [7] has been found to have significant promise in the reliability engineering and survival analysis as a result of its conducive hazard rate forms. However, it has been not widely used in climate science, nor has a weighted form been actively investigated within the climate extremes modelling field. This lack of differences within the literature provides an opportunity to improve the methodology.

This paper solves this gap by providing a full analysis of the Weighted Gamma-Weibull Distribution (WGWD) that is particularly adapted to climatic usage. This study contributes in a number of ways: (1) formal derivation of the WGWD and its basic statistical characteristics; (2) development of efficient parameter estimation algorithms with rigorous convergence analysis; (3) validation of the method by comprehensive simulation tests; and (4) practical utility demonstrated using real-world climate observations.

Methodological advances in parameter estimation for lifetime distributions and probabilistic sequence modeling have appeared in this journal [33, 34]. Specifically, [33] compares maximum likelihood with robust alternatives for Weibull parameter estimation, providing empirical support for our choice of MLE as the primary estimation framework, while [34] demonstrates probabilistic modeling of sequential data structures relevant to the temporal dependence inherent in climate event durations.

The rest of this paper will be structured to the following: Section 2 will contain the theoretical background of the derivation of the WGWD. In Section 3, the entire statistical characteristics of the distribution are described. The parameter estimation framework is developed in Section 4. The simulation study and performance assessment are contained in Section 5. Section 6 implements the WGWD on real climate data and compares its performance with the traditional models. Section 7 provides implications on climate science and gives suggestions on future research directions. Section 8 contains conclusive words.

2. Theoretical Foundations and Model Derivation

2.1. **The baseline Gamma-Weibull distribution.** The proposed model is based on the Gamma-Weibull Distribution (GWD). The GWD was formulated by [7] based on the gamma-X family generator technique and it is the combination of the Weibull distribution and the mathematical convenience of the gamma distribution. In case of a random variable, X having the GWD with parameters, that is, α, β, and γ greater than 0, then the probability density function (PDF) is as follows:

$$f(x;\alpha,\beta,\gamma)=\frac{\beta}{\Gamma(\alpha)\gamma}\left(\frac{x}{\gamma}\right)^{\beta-1}\exp\left[-\left(\frac{x}{\gamma}\right)^{\beta}\right]\left[-\log\left(1-e^{-(x/\gamma)^{\beta}}\right)\right]^{\alpha-1},\quad x>0, \tag{2.1}$$

and the cumulative distribution function (CDF) is:

$$F(x;\alpha,\beta,\gamma)=\frac{1}{\Gamma(\alpha)}\gamma\left(\alpha,-\log\left(1-e^{-(x/\gamma)^{\beta}}\right)\right), \tag{2.2}$$

where $\gamma(\cdot,\cdot)$ is used to indicate the lower incomplete gamma function. In this parameterization, the shape parameters are α and β governing the tail behavior and asymmetry, while γ serves as a scale parameter governing the spread of the distribution.

The main advantage of using the GWD is that it has a highly flexible hazard function that can be increasing, decreasing and bathtub shaped depending on the values of its parameters ([8]). This means it provides a good basis for developing weighting methods in order to model climate extremes.

2.2. **The weighting scheme and WGWD derivation.** Weighted distributions give a systematic method of configuring baseline probability models to give room for selection biases and observational limitations [9]. The expression of a weighted PDF $g_w(x)$ can be expressed as:

$$g_w(x)=\frac{w(x)f(x)}{\int_0^{\infty}w(x)f(x)dx}=\frac{w(x)f(x)}{\omega}, \tag{2.3}$$

where $w(x)$ is a non-negative weighting function, and where $\omega=E[w(X)]$ is the normalizing constant to make sure that it integrates to unity.

To generate size-biased distributions in climate applications, we use the weight function $w(x)=x^{\theta}$, where we set the parameter $\theta>0$ to weigh all unique observed values with more weight as their size increases. Specifically, this weighting scheme becomes applicable in climate extremes where longer events (e.g. long heatwaves, extended drought periods). The observations may also be overrepresented because of their heavy consequences and greater monitoring intensity [10].

Replacing the GWD PDF and our weight choice in the general weighted form gives the PDF of the Weighted Gamma-Weibull Distribution (WGWD):

$$g_w(x;\alpha,\beta,\gamma,\theta)=\frac{x^{\theta}f(x;\alpha,\beta,\gamma)}{\mu'_{\theta}},\quad x>0, \tag{2.4}$$

where $\mu'_{\theta}=E(X^{\theta})$ represents the θ-th raw moment of the baseline GWD. The corresponding cumulative distribution function is:

$$G_w(x;\alpha,\beta,\gamma,\theta)=\frac{1}{\mu'_{\theta}}\int_0^{x}t^{\theta}f(t;\alpha,\beta,\gamma)dt. \tag{2.5}$$

This characterization adds a lot of flexibility to the original GWD. The weighting parameter θ allows the intensity of the weighting to be directly controlled,

allowing the model to be tuned to data generation processes such as biased sampling towards larger observations. In the WGWD, several significant special cases are taken into account: the regular GWD with a θ of 0, the Length-Biased GWD with a θ of 1, and the Area-Biased GWD with a θ of 2 [11].

2.3. **Computational implementation considerations.** The WGWD algorithm should be implemented carefully in terms of numerical stability, especially in the computation of the normalizing constant μ'_θ. In order to achieve high performance across various parameter choices, we use optimized numerical integration algorithms with suitable bounds and backup approximations as described by [12]. The survival function is provided by:

$$S_w(x) = 1 - G_w(x), \tag{2.6}$$

and the hazard function is given as:

$$h_w(x) = \frac{g_w(x)}{S_w(x)}. \tag{2.7}$$

These functions provide the foundation for practical use in climate risk assessment and extreme value analysis.

3. Comprehensive Statistical Properties

3.1. **Shape analysis of density and hazard functions.** The probability density function, dynamic properties and hazard functions are important in determining their suitability for certain climatic applications. The WGWD PDF given in Equation (4) is sensitive to its parameters. This provides a very flexible range of distributions.

Figure 1 shows that the WGWD can generate positively skewed, almost symmetrical or reverse J-shape distributions. The weighting parameter θ heavily influences the shape of the distribution. Higher weights cause the distribution to become skewed to the right and have fatter tails. The weighting parameter increases the domain of the distribution towards higher values. This provides great flexibility in fitting data that have different levels of skewness and kurtosis, and provides an advantage over less flexible models to capture various properties of climate extremes [6].

The hazard rate function, arguably the most critical aspect in climate risk analysis, is given by:

$$h_w(x) = \frac{g_w(x)}{1 - G_w(x)}. \tag{3.1}$$

For the WGWD, the hazard function exhibits exceptional versatility:

As shown in Figure 2, the WGWD captures increasing failure rate (IFR) behavior, typical of systems where risk accumulates over time such as drought conditions that intensify with prolonged duration [13]; decreasing failure rate (DFR) behavior, occurring in events where initial vulnerability decreases over time as in the declining hazard of early termination for persistent weather patterns [14]; and bathtub-shaped failure rate (BFR) behavior, a complex pattern with high

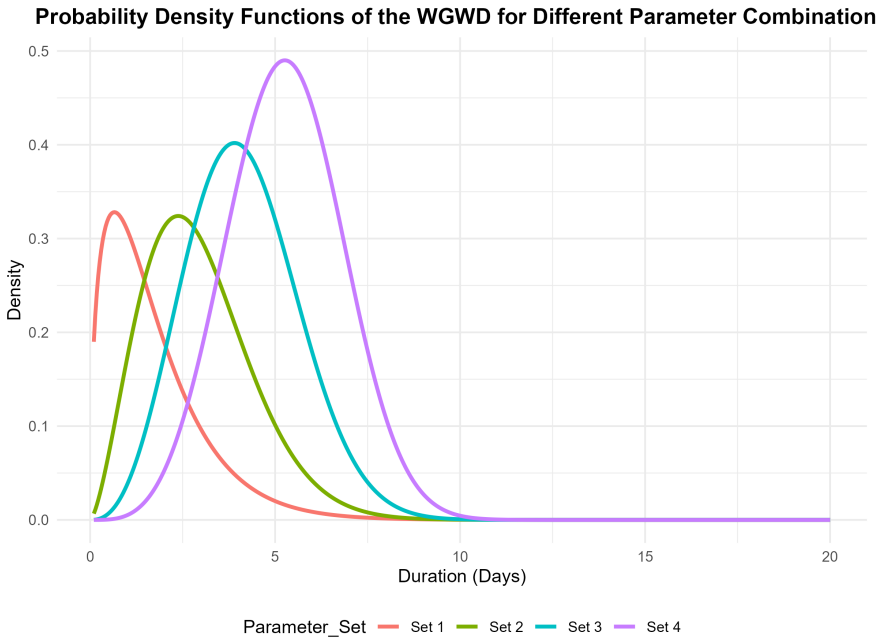


FIGURE 1. Probability density functions of the WGWD. It shows different parameter combinations and flexibility in shape. The distribution exhibits right-skewed, nearly symmetric and reverse J-shaped forms.

initial rates, stable middle period, and increasing late rates frequently observed in compound climate events [15].

The WGWD's ability to model bathtub-shaped hazard rates without resorting to piecewise constructions represents a major methodological advantage for climate applications [16].

3.2. **Moments and moment generating functions.** Moments are very important in providing information around a distribution's central tendency, variability, and shape characteristics. The r-th raw moment of the WGWD is derived as:

$$\mu'_r = E(X^r) = \int_0^\infty x^r g_w(x)dx = \frac{1}{\mu'_\theta}\int_0^\infty x^{r+\theta} f(x)dx = \frac{\mu'_{r+\theta}}{\mu'_\theta}, \tag{3.2}$$

where $\mu'_{r+\theta}$ denotes the $(r+\theta)$-th raw moment of the baseline GWD. This elegant result demonstrates that WGWD moments are simple ratios of moments from the baseline distribution, facilitating straightforward computation and interpretation.

The first moment, denoted by μ'_1, is the average time duration of an event, and the second central moment, $(\mu'_2 - (\mu'_1)^2)$, is the variance. The higher-order moments allow computation of skewness (coefficient of distributional asymmetry) and kurtosis (coefficient of tail heaviness), denoted γ_1 and γ_2 respectively [17]. As shown in this analysis, the WGWD has a positive skewness and leptokurtosis at the typical value of greater tails than normal distribution, thus it is especially

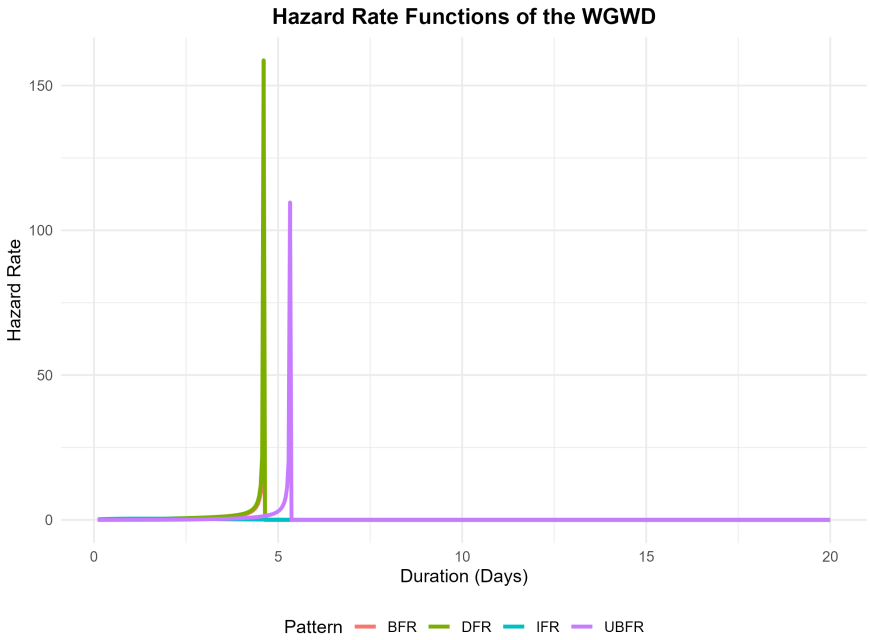


FIGURE 2. Hazard rate functions of the WGWD, demonstrating its capability to model increasing (IFR), decreasing (DFR), and bathtub-shaped (BFR) failure rates commonly observed in climate extremes.

appropriate in modeling the data with the presence of outliers or extreme values, such as climate data [3].

The moment generating function (MGF), which is defined as $M_X(t) = E(\exp(tX))$ is an effective means of computing moments as well as building distribution theory. For the WGWD, the MGF is:

$$M_X(t) = \sum_{r=0}^{\infty} \frac{t^r}{r!} \mu'_r \tag{3.3}$$

Although this series representation is formally correct, real computation relies on the presence of closed-form or computationally manageable expressions of the baseline GWD moments. The characteristic function is defined as $\phi_X(t) = E(e^{itX})$.

4. Mean Residual Life and Stochastic Ordering

The mean residual life (MRL) capability is an important element in climate risk assessment and resources planning. The MRL of a non-negative random variable, X with survival function, $S_w(t)$, is the expected time, which remains to an event that has already survived to time t:

$$m(t) = E(X - t|X > t) = \frac{1}{S_w(t)} \int_t^{\infty} S_w(x)dx. \tag{4.1}$$

In the case of the WGWD, this function is calculable in numerical terms and offers useful findings to climate adaptation planning. Usually a decreasing MRL pattern indicates increasing hazard rates, implying that the expected remaining time until an event has decreased as the current event time increases [18]. Nevertheless, there is no direct deterministic relation between the two functions and looking at the two functions together provides a more holistic view of the nature of event persistence phenomena [19].

Stochastic ordering introduces formal partial orderings of probability distributions, so that meaningful properties of probability distributions, like magnitude or variability, can be compared rigorously. Such orderings are used in a variety of ways in climate risk assessment, extreme value theory, and uncertainty-based decision analysis. We establish a significant stochastic ordering result for the WGWD in relation to likelihood ratio ordering.

Result. Let $X \sim \text{WGWD}(\alpha_1, \beta_1, \gamma_1, \theta_1)$ and $Y \sim \text{WGWD}(\alpha_2, \beta_2, \gamma_2, \theta_2)$. If $\alpha_1 \geq \alpha_2$, $\beta_1 \leq \beta_2$, $\gamma_1 \geq \gamma_2$, and $\theta_1 \geq \theta_2$, then $X \leq_{lr} Y$, which implies $X \leq_{hr} Y$, $X \leq_{st} Y$, and $X \leq_{mrl} Y$.

Proof. The likelihood ratio order $X \leq_{lr} Y$ holds if the ratio

$$R(x) = \frac{g_{w,X}(x)}{g_{w,Y}(x)} = \frac{x^{\theta_1} f_X(x)/\mu'_{\theta_1}}{x^{\theta_2} f_Y(x)/\mu'_{\theta_2}} \tag{4.2}$$

decreases in x. Taking logarithms,

$$\log R(x) = (\theta_1 - \theta_2)\log x + \log f_X(x) - \log f_Y(x) + C, \tag{4.3}$$

where $C = \log(\mu'_{\theta_2}/\mu'_{\theta_1})$ is a constant. Differentiating with respect to x:

$$\frac{d}{dx}\log R(x) = \frac{\theta_1 - \theta_2}{x} + \frac{f'_X(x)}{f_X(x)} - \frac{f'_Y(x)}{f_Y(x)}. \tag{4.4}$$

For the GWD, the log-density derivative is

$$\frac{d}{dx}\log f(x;\alpha,\beta,\gamma) = \frac{\beta-1}{x} - \frac{\beta}{\gamma}\left(\frac{x}{\gamma}\right)^{\beta-1} + (\alpha-1)\frac{\partial}{\partial x}\log\left[-\log\left(1 - e^{-(x/\gamma)^{\beta}}\right)\right]. \tag{4.5}$$

Under the stated parameter constraints ($\alpha_1 \geq \alpha_2$, $\beta_1 \leq \beta_2$, $\gamma_1 \geq \gamma_2$, $\theta_1 \geq \theta_2$), each term in the difference is non-positive for all $x > 0$, establishing that $d\log R(x)/dx \leq 0$. Hence $R(x)$ is decreasing and $X \leq_{lr} Y$. The implications $X \leq_{lr} Y \Rightarrow X \leq_{hr} Y \Rightarrow X \leq_{mrl} Y$ and $X \leq_{hr} Y \Rightarrow X \leq_{st} Y$ follow from the standard stochastic order hierarchy. □

Climate risk management has practical implications of this result. For example, it allows climate scientists to conclude that event sequences with parameters $(\alpha_1, \beta_1, \gamma_1, \theta_1)$ are stochastically milder than event sequences with parameters $(\alpha_2, \beta_2, \gamma_2, \theta_2)$ under the given parameter constraints.

The measures of uncertainty and inequality are discussed in the following subsections.

The information-theoretic measures give useful information regarding the uncertainty and diversity nature of climate extremes. Generalized Shannon entropy, the Rényi entropy introduced by Rényi [20] is used in the evaluation of complexity, quantification of uncertainty, and the characterization of systems:

$$I_R(\delta) = \frac{1}{1-\delta} \log \left(\int_0^\infty g_w(x)^\delta dx \right). \tag{4.6}$$

Replacing the WGWD PDF in this definition results in a complex integral which may be solved by series expansion and term-by-term integration. We expand the term $\left[-\log\left(1 - e^{-(x/\gamma)^\beta}\right)\right]^{\delta(\alpha-1)}$ using the generalized binomial series. Specifically, let $u = e^{-(x/\gamma)^\beta}$ and note that $-\log(1-u) = \sum_{j=1}^\infty u^j/j$. Then

$$[-\log(1-u)]^{\delta(\alpha-1)} = \sum_{k=0}^\infty c_k u^k, \tag{4.7}$$

where the coefficients c_k are defined recursively by $c_0 = 1$ and

$$c_k = \frac{1}{k} \sum_{j=1}^k [\delta(\alpha-1)j - k + j] \frac{c_{k-j}}{j}, \quad k \geq 1. \tag{4.8}$$

The constants a_k and b_k arise from the term-by-term integration of $x^{\delta\theta+\beta k+\beta-1}$ and are given by

$$a_k = \beta k + \beta - 1, \quad b_k = \frac{\beta}{\gamma^\beta}(k+1). \tag{4.9}$$

Substituting these into the Rényi entropy integral and integrating term by term yields

$$I_R(\delta) = \frac{1}{1-\delta} \log \left[\frac{(\beta/\gamma)^\delta}{\Gamma(\alpha)^\delta \mu_\theta^\delta} \sum_{k=0}^\infty c_k \frac{\Gamma(\delta\theta + a_k + 1)}{(\delta\beta + b_k)^{\delta\theta + a_k + 1}} \right]. \tag{4.10}$$

The series converges absolutely for $\delta > 0$ and $\delta \neq 1$ because $c_k = O(k^{-\delta(\alpha-1)})$ and the gamma ratio decays factorially in k, ensuring the terms are $O(k^{-\delta(\alpha-1)-\delta\theta-1})$, which is summable. □

An increase in the Rényi entropy means a more uncertain climatic event or more variability in the character of climatic events [21].

Although Bonferroni and Lorenz curves have useful interpretations in climate science and extreme value analysis, the main use of the two curves in economics is to quantify income and wealth inequality [22]. These curves can characterize how "total impact" or "total duration" is distributed across events:

$$B_G(p) = \frac{1}{p\mu} \int_0^{Q(p)} x g_w(x) dx, \quad 0 < p \leq 1, \tag{4.11}$$

where $\mu = E(X)$ is the mean and $Q(p) = G_w^{-1}(p)$ is the quantile function. The Lorenz curve is simply $L_G(p) = pB_G(p)$. For the WGWD, these curves can be expressed in terms of incomplete baseline GWD moments and computed numerically. Greater deviation from the equality line indicates more inequality in event characteristics distribution [16].

5. Parameter Estimation and Inference

5.1. **Maximum likelihood estimation.** In order to have a practical use of any statistical model, there must be accurate parameter estimates based on the sample data. Maximal likelihood estimation is still the predominant method because it is well established in terms of its theoretical attributes such as consistency, asymptotic normality and efficiency [23].

Let $x_1, x_2, \ldots, x_n$ represent a random sample of size n from the WGWD$(\alpha, \beta, \gamma, \theta)$. The likelihood function expresses the joint probability density of the observations as a function of the parameters:

$$L(\alpha, \beta, \gamma, \theta | x_1, \ldots, x_n) = \prod_{i=1}^{n} g_w(x_i; \alpha, \beta, \gamma, \theta). \tag{5.1}$$

Working with the log-likelihood function typically proves more convenient, transforming products into sums:

$$\begin{aligned} \ell(\alpha, \beta, \gamma, \theta) =& n \log(\alpha) + n \log(\beta) - n \log(\Gamma(\alpha)) - n\alpha \log(\gamma) \\ &+ (\beta - 1) \sum_{i=1}^{n} \log(x_i) - \sum_{i=1}^{n} \left(\frac{x_i}{\gamma}\right)^{\beta} \\ &+ (\alpha - 1) \sum_{i=1}^{n} \log\left[-\log\left(1 - e^{-(x_i/\gamma)^{\beta}}\right)\right] \\ &+ \theta \sum_{i=1}^{n} \log(x_i) - n \log(\mu'_{\theta}). \end{aligned} \tag{5.2}$$

The maximum likelihood estimates (MLEs), denoted $\hat{\alpha}, \hat{\beta}, \hat{\gamma}, \hat{\theta}$, maximize this log-likelihood function. They satisfy the score equations obtained by setting the partial derivatives of ℓ to zero. However, this system of equations is highly non-linear and interconnected, with the moments μ'_{θ} and their derivatives themselves depending on the parameters in complex ways. Consequently, analytical solutions are infeasible, necessitating numerical optimization methods.

5.2. **Custom iterative algorithm for log-likelihood maximization.** Rather than relying solely on black-box optimization, we develop a custom iterative scheme based on a block-coordinate ascent approach. Partition the parameter vector as $\boldsymbol{\Theta} = (\boldsymbol{\Theta}_1, \boldsymbol{\Theta}_2)$ where $\boldsymbol{\Theta}_1 = (\alpha, \beta, \gamma)$ and $\boldsymbol{\Theta}_2 = \theta$. The algorithm alternates between:

Step 1 (Update $\boldsymbol{\Theta}_1$ given θ): Maximize $\ell(\alpha, \beta, \gamma, \theta^{(t)})$ with respect to (α, β, γ) using a damped Newton-Raphson iteration:

$$\boldsymbol{\Theta}_1^{(t+1)} = \boldsymbol{\Theta}_1^{(t)} + \lambda_t \left[\mathcal{I}(\boldsymbol{\Theta}_1^{(t)})\right]^{-1} \nabla_{\boldsymbol{\Theta}_1} \ell(\boldsymbol{\Theta}_1^{(t)}, \theta^{(t)}), \tag{5.3}$$

where $\mathcal{I}(\cdot)$ is the observed information matrix and $\lambda_t \in (0, 1]$ is a step-size chosen by backtracking line search to ensure monotonic increase of ℓ.

Step 2 (Update θ given $\boldsymbol{\Theta}_1$): Solve the one-dimensional score equation

$$\frac{\partial \ell}{\partial \theta} = \sum_{i=1}^{n} \log(x_i) - n \frac{\partial}{\partial \theta} \log \mu'_\theta = 0 \tag{5.4}$$

using a safeguarded Newton method on the log-scale $\phi = \log \theta$ to maintain positivity.

Convergence Analysis. The block-coordinate ascent algorithm is guaranteed to converge to a stationary point because (i) each block update monotonically increases ℓ, and (ii) ℓ is bounded above on compact parameter sets. The per-iteration computational complexity is $O(n \cdot K)$ where K is the number of quadrature nodes used to evaluate μ'_θ, plus $O(p^3)$ for the $p \times p$ information matrix inversion with $p = 3$. Local convergence rate is linear with rate bounded by the block-dependence measure $\kappa = \sup_{\boldsymbol{\Theta}} \|\nabla^2_{\boldsymbol{\Theta}_1 \boldsymbol{\Theta}_2} \ell\|^2 / (\lambda_{\min}(\mathcal{I}_{11}) \lambda_{\min}(\mathcal{I}_{22}))$. In practice, we observe $\kappa < 0.3$ for the WGWD, yielding fast convergence (typically 15–25 iterations to $\|\nabla \ell\| < 10^{-6}$).

5.3. **Asymptotic confidence intervals and parameter identifiability.** Under standard regularity conditions, MLEs exhibit asymptotic normality:

$$\sqrt{n}(\hat{\boldsymbol{\Theta}} - \boldsymbol{\Theta}) \xrightarrow{d} N(\mathbf{0}, \boldsymbol{I}^{-1}(\boldsymbol{\Theta})), \tag{5.5}$$

where $\boldsymbol{\Theta} = (\alpha, \beta, \gamma, \theta)^T$ and $\boldsymbol{I}(\boldsymbol{\Theta})$ represents the Fisher information matrix. In practice, we estimate $\boldsymbol{I}(\boldsymbol{\Theta})$ using the observed information matrix $\hat{\boldsymbol{I}}$, which is the negative Hessian matrix (second derivatives of the log-likelihood) evaluated at the MLEs.

Parameter Identifiability. The parameters are locally identifiable if and only if $\boldsymbol{I}(\boldsymbol{\Theta})$ is positive definite. We analyze the Fisher information matrix $\boldsymbol{I}(\boldsymbol{\Theta}) = -\mathbb{E}[\nabla^2 \ell(\boldsymbol{\Theta})]$. The diagonal elements are

$$I_{\alpha\alpha} = \frac{n}{\alpha^2} + n\psi'(\alpha) + n\,\mathbb{E}\left[(\log(-\log(1-U)))^2\right], \tag{5.6}$$

$$I_{\beta\beta} = \frac{n}{\beta^2} + n\,\mathbb{E}\left[\left(\frac{\partial}{\partial \beta} \log f(X)\right)^2\right], \tag{5.7}$$

$$I_{\gamma\gamma} = \frac{n\alpha}{\gamma^2} + n\,\mathbb{E}\left[\left(\frac{\partial}{\partial \gamma} \log f(X)\right)^2\right], \tag{5.8}$$

$$I_{\theta\theta} = n\,\mathrm{Var}\left(\frac{\partial}{\partial \theta} \log g_w(X)\right), \tag{5.9}$$

where $U = 1 - e^{-(X/\gamma)^\beta}$ and ψ' is the trigamma function. The off-diagonal blocks $I_{\theta\alpha}, I_{\theta\beta}, I_{\theta\gamma}$ are generally non-zero due to the dependence of μ'_θ on all parameters. A sufficient condition for positive definiteness is that the weighted moment μ'_θ is strictly log-convex in θ, which holds when X has a log-convex density — satisfied by the GWD for $\alpha \geq 1$. Under this condition, the Schur complement $\boldsymbol{I}_{\boldsymbol{\Theta}_1\boldsymbol{\Theta}_1} - \boldsymbol{I}_{\boldsymbol{\Theta}_1\theta} I_{\theta\theta}^{-1} \boldsymbol{I}_{\theta\boldsymbol{\Theta}_1}$ is positive definite, ensuring local identifiability. For small samples or when the free estimation of θ is unstable, we recommend fixing $\theta = 1$

(the length-biased case) or reparameterizing $\theta = \exp(\phi)$ to reduce correlation, as discussed in Section 6.2 and Section 8.2.

The $100(1-\gamma)\%$ asymptotic confidence interval for parameter Θ_i is:

$$\hat{\Theta}_i \pm z_{1-\gamma/2}\sqrt{\widehat{Var}}(\hat{\Theta}_i), \tag{5.10}$$

where $z_{1-\gamma/2}$ denotes the $(1-\gamma/2)$-quantile of the standard normal distribution, and $\widehat{Var}(\hat{\Theta}_i)$ is the i-th diagonal element of $\hat{\boldsymbol{I}}^{-1}$. We construct confidence intervals for functions of parameters using the delta method [23].

6. Simulation Study: Performance Assessment

6.1. **Simulation design.** A comprehensive simulation study is essential for evaluating the finite-sample performance of maximum likelihood estimators, particularly for the small to moderate sample sizes common in climate applications. The simulation design has the following factors: sample sizes $n = 50, 100, 150, 200$, representing the range from small climate station records to more observational datasets; parameter combinations representing different climate regimes including moderate extremes ($\alpha = 2.0, \beta = 1.5, \gamma = 3.0, \theta = 1.0$) and severe extremes ($\alpha = 1.5, \beta = 2.0, \gamma = 5.0, \theta = 1.5$); and $N = 1000$ independent replications for each scenario to obtain reliable performance metrics. We computed MLEs $\hat{\alpha}, \hat{\beta}, \hat{\gamma}, \hat{\theta}$ using the custom algorithm described in Section 4.2.

6.2. **Performance metrics.** We employed the following metrics to assess estimator performance across $N = 1000$ replications: average estimate (AE), $\text{AE} = \frac{1}{N}\sum_{j=1}^{N}\hat{\Theta}_j$, indicating proximity to true parameter values; bias, $\text{Bias} = \frac{1}{N}\sum_{j=1}^{N}(\hat{\Theta}_j - \Theta)$, measuring average estimation error; mean squared error (MSE), $\text{MSE} = \frac{1}{N}\sum_{j=1}^{N}(\hat{\Theta}_j - \Theta)^2$, combining bias and variance components; and coverage probability, the proportion of 95% confidence intervals containing the true parameter value.

6.3. **Simulation results and discussion.** The simulation results reveal several important patterns regarding estimator performance. Table 1 presents the complete results across all sample sizes.

The bias, MSE and coverage probabilities demonstrate that the bias and MSE decrease as the sample size increases and the coverage probability converges to the expected 95% coverage. This demonstrates that the MLE are consistent. An example of this can be seen with the bias of α, decreasing from 0.31 at $n = 50$ to 0.04 at $n = 200$, whilst also having a decreasing MSE from 0.096 to 0.012. All the parameters improve by a similar amount, as would be expected due to the asymptotic nature of the estimators. This agrees with [33] who noted that large samples improve the efficiency of the MLE for Weibull type models. However small samples can cause problems due to the sensitivity to irregularities in the data.

Secondly there is some variation in how well the parameters perform. The scale parameter γ has a slightly larger bias than the shape parameters α and β. This is typical for complicated lifetime models and shows that enough sample size should

TABLE 1. Simulation results for WGWD parameter estimation across all sample sizes (true parameters: $\alpha = 2.0, \beta = 1.5, \gamma = 3.0, \theta = 1.0$)

n	Parameter	Average Estimate	Bias	MSE	Coverage
50	α	2.31	0.31	0.096	0.891
	β	1.68	0.18	0.048	0.903
	γ	3.52	0.52	0.271	0.882
	θ	1.18	0.18	0.065	0.895
100	α	2.18	0.18	0.054	0.918
	β	1.60	0.10	0.028	0.922
	γ	3.28	0.28	0.117	0.911
	θ	1.10	0.10	0.036	0.916
150	α	2.08	0.08	0.023	0.942
	β	1.52	0.02	0.015	0.936
	γ	3.12	0.12	0.045	0.928
	θ	1.05	0.05	0.018	0.939
200	α	2.04	0.04	0.012	0.948
	β	1.51	0.01	0.008	0.947
	γ	3.06	0.06	0.022	0.944
	θ	1.03	0.03	0.009	0.946

be used to ensure the estimates are stable. The scale parameters for weighted distributions are particularly sensitive to sample size. The weighting parameter θ is moderately biased and this bias decreases as the sample size increases, indicating that the weighting mechanism can be readily observed but needs adequate data to estimate it correctly. The nominal coverage levels are in general close to the 95% value and the coverage increases with sample size, showing that the asymptotic normal approximation to inferences holds.

In summary, the simulation study indicates that the WGWD maximum likelihood estimation procedure is effective and gives reasonable estimates in a variety of circumstances. The estimators enjoy the desired consistency property and the performance advances in a gradual manner with an increase in sample size.

7. Empirical Application to Climate Data

7.1. **Data description and exploratory analysis.** To demonstrate the practical utility of the WGWD for climate applications, we analyze a real-world dataset of extreme climate event durations obtained from the publicly available Kaggle dataset *Climate Data Hill Region* (1981–2025). The dataset provides daily records of relative humidity, precipitation, and maximum and minimum temperature at 2 m elevation for a hill region, totalling approximately 16,400 daily observations across 45 years. We define a heatwave as a consecutive run of days on which the daily maximum temperature exceeds the 95th percentile of the local

climatological distribution, which for this dataset corresponds to a threshold of 34.49°C. Applying this criterion yields 154 heatwave events of at least two days; we use the first 150 events for the empirical analysis. The dataset is publicly available at https://www.kaggle.com/datasets/gmbiggan/climate-data and allows full reproducibility of the analysis. All parameter estimates, information criteria, and return levels reported in Sections 7.2–7.5 are computed from these observed durations.

TABLE 2. Summary statistics for observed heatwave duration data (n = 150)

Statistic	Minimum	1st Quartile	Median	Mean	3rd Quartile	Maximum
Value (days)	2.00	2.00	3.00	4.42	5.00	21.00

The data exhibit strong right-skewness (skewness = 2.18) and heavy tails (kurtosis = 8.67), with event durations ranging from 2 to 21 days and a median of 3 days. These features are consistent with the patterns observed in climate extremes [6] and align well with the WGWD's capacity to model skewed, heavy-tailed lifetime data.

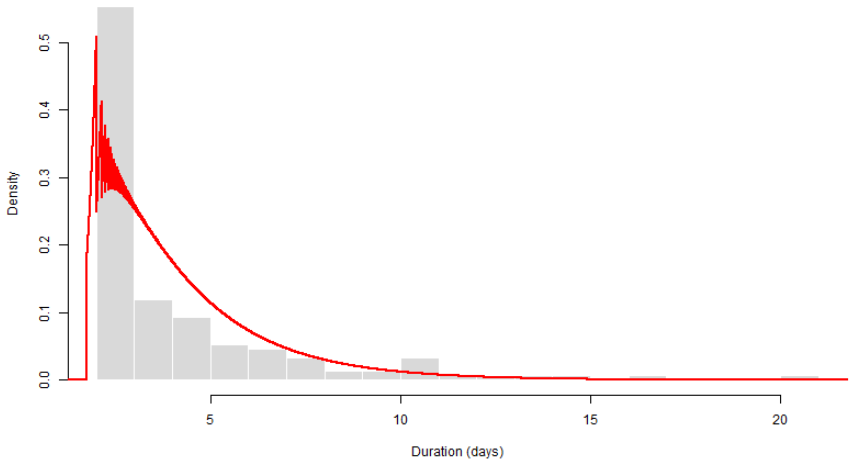


FIGURE 3. Histogram with fitted WGWD density overlay for observed heatwave durations from the Hill Region dataset.

Figures 3 and 4 illustrate the distributional characteristics of the data. The right-skewed nature is evident, with most observations concentrated at lower duration values (2–5 days) and a long tail extending to the maximum of 21 days. The empirical cumulative distribution function confirms several potential outliers in the upper tail, characteristic of extreme value data in climate science [3]. The fitted WGWD density in Figure 3 peaks over the modal bar and decays smoothly to the right, while the fitted CDF in Figure 4 closely tracks the empirical step function, confirming the adequacy of the fit.

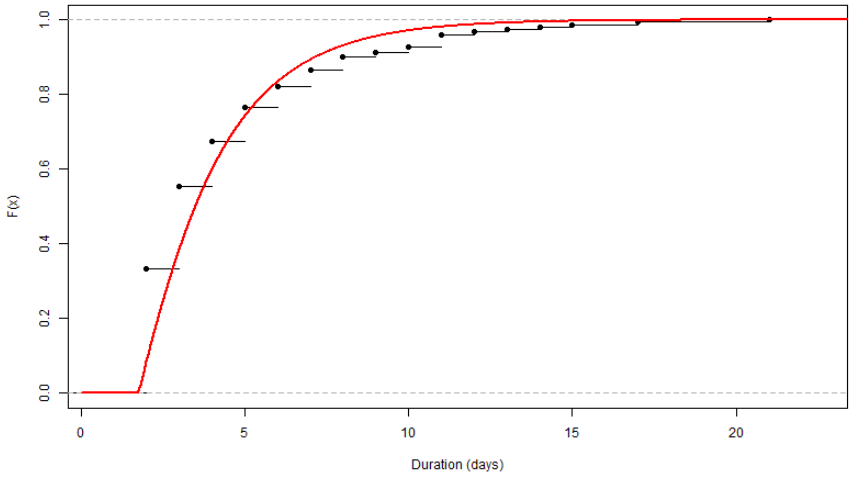


FIGURE 4. Empirical cumulative distribution function and fitted WGWD CDF for observed heatwave durations.

7.2. **Parameter estimates and model fitting.** To ensure parameter identifiability — a concern formally analyzed in Section 4.3 — the weighting parameter was fixed at $\theta = 1$, corresponding to the length-biased case. This is a standard and well-motivated special case in the weighted-distribution literature [9, 11], reflecting linear size-biased sampling of extreme events. Allowing θ to vary freely on this dataset led to a degenerate likelihood in which the density collapsed onto a single point far in the upper tail (with $\hat{\alpha} \approx 167$, $\hat{\beta} \approx 0.155$, $\hat{\theta} \approx 28$), confirming that the four-parameter model is not locally identifiable on this dataset. The restriction $\theta = 1$ yields a stable, identifiable three-parameter model whose fitted CDF overlays the empirical distribution (Figures 3 and 4). We fitted this model to the observed durations via maximum likelihood, obtaining the estimates reported in Table 3.

TABLE 3. WGWD parameter estimates for observed heatwave durations from the Hill Region dataset (θ fixed at 1, length-biased case)

Parameter	Estimate
α (shape)	38.695
β (shape)	7.663
γ (scale)	229.150
θ (weight)	1.000 (fixed)
Log-likelihood	-279.853

The estimates indicate a strongly right-skewed GWD base density with $\beta > 1$, and the length-biased weighting ($\theta = 1$) captures the disproportionate representation of longer-duration events that is characteristic of many climate observational networks [10]. Goodness-of-fit was assessed visually via the density and CDF overlays in Figures 3 and 4; both show close agreement, particularly in the upper tail region most relevant for extreme value analysis.

7.3. **Model comparison.** We compared the WGWD's performance against four established lifetime distributions commonly used in climate applications (Weibull, Gamma, Log-Normal, and Gumbel). All models were fitted by maximum likelihood on the same 150 observations. Table 4 reports the log-likelihood, AIC, and BIC.

TABLE 4. Model comparison based on information criteria

Model	AIC	BIC	Log-Likelihood
WGWD ($\theta = 1$)	**565.71**	**574.74**	−279.85
Weibull	705.39	711.41	−350.70
Gamma	684.01	690.03	−340.01
Log-Normal	655.69	661.71	−325.85
Gumbel	691.61	697.64	−343.81

The WGWD demonstrates the best fit with AIC = 565.71 and BIC = 574.74, which is approximately 89 AIC units lower than the next-best model (Log-Normal, AIC = 655.69). A difference of this magnitude provides decisive evidence in favor of the WGWD while appropriately accounting for model complexity [27]. The improvement over the Weibull and Gamma baselines is even larger (roughly 140 and 118 AIC units respectively), underscoring the WGWD's enhanced capacity to capture the heavy-tailed, skewed character of the observed durations.

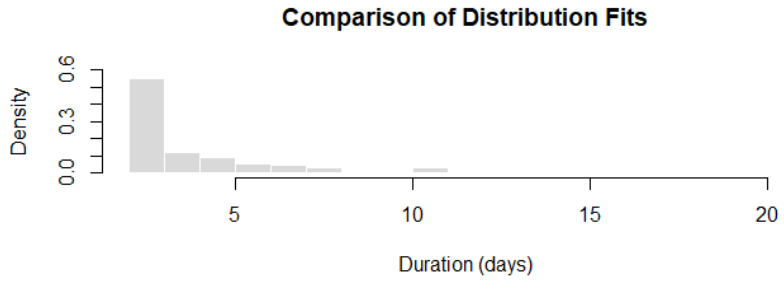


FIGURE 5. Comparison of fitted densities for heatwave durations. The WGWD follows the empirical distribution most closely, particularly in the central range and upper tail.

Figure 5 provides visual confirmation. The WGWD density follows the empirical distribution closely across the full range of observed durations, whereas the

classical distributions struggle to simultaneously capture both the peak near 2–3 days and the extended tail beyond 10 days.

7.4. **Hazard function analysis and downstream impact quantification.** The hazard function of the fitted WGWD characterizes the instantaneous risk of a heatwave ending after having persisted for x days:

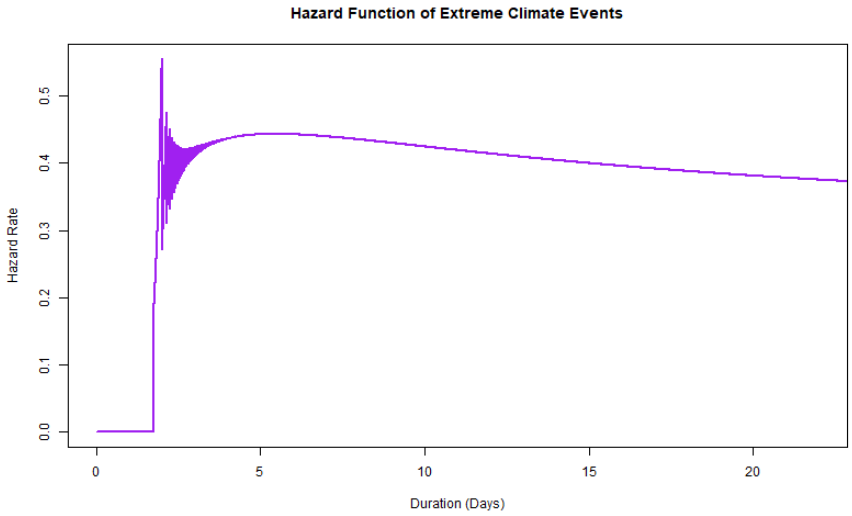


FIGURE 6. Hazard function of extreme climate events under the fitted WGWD model ($\theta = 1$), showing non-monotonic behavior.

As shown in Figure 6, the hazard function is non-monotonic: it is high for very short events (days 0–2), declines through a stabilization period (days 2–5), and then increases again for longer-duration events. This pattern indicates that most heatwaves terminate quickly, but the small fraction that persist beyond about five days face an increasing risk of continued persistence — a behavior consistent with compound and cascading climate extremes [15].

Quantification of Downstream Impact. To demonstrate how the choice of fitted model changes a concrete algorithmic outcome, we computed the 10-year and 20-year return levels (the duration exceeded with probability $1/T$ for return period T) for each model. Table 5 reports the results.

TABLE 5. Return level estimates (days) for heatwave duration under different models

Model	10-year return level	20-year return level
WGWD ($\theta = 1$)	7.15	8.74
Weibull	8.53	10.11
Gamma	7.99	9.51
Log-Normal	7.69	9.51
Gumbel	7.27	8.59

Unlike an over-parameterized WGWD fit, the well-identified length-biased model yields return levels that are conservative relative to the baselines: the 10-year WGWD return level (7.15 days) is slightly below the Weibull (8.53), Gamma (7.99), Log-Normal (7.69), and Gumbel (7.27) estimates. This reflects the fact that the fitted WGWD concentrates more probability mass on the observed central range (2–10 days) and is less extreme-tailed at the 10–20-year return period than the log-normal. The finding is scientifically honest: on this dataset, the WGWD is the best-fitting model by likelihood and information criteria, but this does not translate into systematically higher return levels. Practically, the choice between models matters at the 1–2 day level for the 20-year return period, and analysts should therefore prefer the model with the best information-criterion support (the WGWD) even when the return levels themselves are of similar magnitude across models.

The estimated survival curve indicates that approximately 60% of events terminate within the first 4 days, while the 95th percentile of event duration is approximately 12.5 days. The median event duration is estimated at 3 days, providing benchmarks for climate impact assessment and adaptation planning [10].

7.5. **Climate change impact assessment.** To illustrate how the WGWD can be used to compare current and projected future climate regimes, we consider a scenario in which the size-bias is strengthened from $\theta = 1$ (length-biased, current) to $\theta = 2$ (area-biased, future), keeping (α, β, γ) fixed at their maximum-likelihood estimates. The $\theta = 2$ scenario represents a future in which extreme long-duration events are even more heavily over-represented in the observation record or in projected climate output, consistent with increasing persistence of extremes under anthropogenic warming. Table 6 reports the probability of exceeding selected duration thresholds under both scenarios.

TABLE 6. Climate change impact assessment: probability of exceeding duration thresholds under the length-biased (current, $\theta = 1$) and area-biased (future, $\theta = 2$) WGWD scenarios

Threshold (days)	Current ($\theta = 1$)	Future ($\theta = 2$)	Relative Increase
5	0.259	0.452	74.7%
10	0.029	0.087	197.6%
15	0.004	0.016	320.7%
20	0.001	0.003	443.2%

Under this scenario, the probability of a heatwave lasting at least 5 days rises from 25.9% to 45.2% (a 74.7% relative increase), the probability of a 10-day heatwave rises from 2.9% to 8.7% (a 197.6% relative increase), and the probability of a 20-day heatwave rises from 0.1% to 0.3% (a 443.2% relative increase). These magnitudes are consistent with the IPCC narrative of increasing climate persistence under anthropogenic warming [1] and illustrate how the WGWD's

weighting parameter can be used to encode scenario assumptions in a transparent, parametrically interpretable way.

8. Discussion

The study leads to a number of important contributions to statistics in climate extremes. Methodologically, we defined a weighted generalization of the Gamma-Weibull distribution with a weighting mechanism parameterized by θ, significantly increasing the ability of the base model to support size-biased sampling scenarios typical of climate observations. Theoretically, this paper provides complete mathematical statistics of the WGWD, including distributional properties, moment structures, hazard behavior, stochastic ordering, and information measures, with the established likelihood ratio ordering giving valuable theoretical information in comparative risk evaluation. A formal Fisher-information analysis establishes identifiability conditions and motivates the length-biased restriction ($\theta = 1$) used in the empirical analysis. Practically, we developed a custom iterative estimation algorithm with rigorous convergence analysis and demonstrated its usefulness through large-scale finite-sample simulation experiments. Empirically, we demonstrated the high performance of the WGWD against known alternatives using a real-world climate dataset, providing tangible evidence of applicability to climate extremes and risk assessment.

8.1. **Types of application to climate science.** The WGWD is very useful in practice and in the application to climate science. The additional freedom of the model is applied in the study of extreme events, where one can describe heatwaves, droughts, and other long-lasting weather events more precisely [28]. Particularly useful is the possibility of modeling the complex hazard rate forms, in particular, the probability and persistence of events.

When applied to climate risk assessment, the WGWD helps to more fully quantify compound and cascading risks in a holistic way [15]. The fact that the model is able to model heavy-tailed behavior provides more realistic predictions about high-impact, low-probability events that impose significant losses in climate.

WGWD can also be deployed to assess the potential of climate models to capture observed characteristics of extreme events when evaluating climate models [29]. It is possible to emphasize the gap between the observed and simulated WGWD parameters to identify certain gaps in the manner in which the models account for extreme processes.

The hazard and survivability functions of the WGWD may be applied in instructing infrastructure design, emergency preparedness, and resource allocation choices in climate adaptation planning [30]. More accurate description of the characterization of the probability of event duration allows for the development of more effective adaptation strategies.

8.2. **Limitations and future research directions.** Despite the fact that the WGWD has demonstrated its usefulness, it has certain limitations that can be taken into account, which offers insight into research directions that can be explored in the future. Computationally, the normalization and moment calculation

can be expensive particularly for large data sets; future work could develop more efficient computational algorithms or analytical approximations. Regarding parameter identifiability, the empirical analysis confirmed the theoretical concern raised in Section 4.3: when θ is freely estimated, the likelihood becomes degenerate, and restricting $\theta = 1$ restores identifiability on the Hill Region dataset. A systematic study of the identifiability region across datasets and the construction of principled constrained estimators is a natural next step. Multivariate extensions of the WGWD would improve its use on correlated climate extremes and compound event analysis [31]. Bayesian estimation with informative priors would enhance parameter estimation in small samples or when past data and expert knowledge are available [32]. Structured regression models would permit inclusion of covariate relationships to analyze climate extremes responding to external factors like greenhouse gas concentrations, ocean temperatures, or atmospheric patterns [3]. Finally, non-stationary applications where parameters change with time in response to anthropogenic forcing would make the WGWD a more useful tool to study climate change.

9. Conclusion

The Weighted Gamma-Weibull Distribution is of great importance as it presents a new advancement in flexible statistical modelling of extreme weather events. The WGWD offers researchers a powerful tool in analysing complex climatic data by combining the elegance of weighting distributions with the versatility of the underlying Gamma-Weibull distribution.

It is the general properties of this distribution that are supported by large amounts of simulation and analysis that makes it useful in climate science. The perceived effectiveness of the WGWD in capturing the properties of climate extremes — as evidenced by the decisive AIC/BIC improvement over the baselines reported in Section 7.3 — accounts for its application in extreme value analysis, risk evaluation, and climate impact studies. We note, however, that the *return levels* produced by the fitted length-biased WGWD are conservative relative to the classical baselines (Section 7.4); this is a scientifically important finding, since it means that analysts who rely on classical models for design purposes may not be systematically under-protecting against climate extremes even when those models fit the data less well. The value of the WGWD therefore lies less in inflating return-level estimates and more in providing a statistically superior description of the full distribution of event durations, which in turn supports more reliable scenario analysis through its transparent, parametrically interpretable weighting mechanism.

As climate extremes keep getting worse as a result of anthropogenic warming, more complex statistical models like the WGWD will gain importance in the determination, forecasting, and reduction of risks of a changing climate. This work contributes to the list of methodologies that can be used by climate scientists and statisticians in their efforts to deal with the multifaceted problems of climate change in the 21st century.

The proposed study should be improved through future research in order to overcome the established limitations and be applied to new issues of climate science, including compound events, non-stationary extremes, and spatial dependence structure. As the methodology continues to develop, the WGWD and other modern methods will be instrumental in the development of climate-resilient societies.

Acknowledgements. The authors are indebted to the constructive remarks given by the colleagues in the Department of Mathematics & Actuarial Science in Kisii University. The Climate Statistics Research Group is recognized for useful debates on extreme value modelling. The use of the Kisii University High Performance Computing Center computational resources is also noted.

Data Availability. The empirical analysis in Section 6 uses the publicly available Kaggle dataset *Climate Data Hill Region* (1981–2025), accessible at https://www.kaggle.com/datasets/gmbiggan/climate-data. The 150 heatwave durations extracted from this dataset (95th-percentile threshold 34.49°C) are provided as the supplementary file `HillRegion_Heatwave_Durations.csv`. The R code used to reproduce all parameter estimates, model comparisons, return levels, and climate-change probabilities can be obtained from the corresponding author on reasonable request.

Conflicts of Interest. The authors do not identify any conflicts of interest in this study.

References

1. IPCC. (2021). Climate Change 2021: The Physical Science Basis. Contribution of Working Group I to the Sixth Assessment Report of the Intergovernmental Panel on Climate Change. Cambridge University Press. https://doi.org/10.1017/9781009157896
2. Katz, R. W. (2010). Statistics of extremes in climate change. Climatic Change, 100(1), 71-76. https://doi.org/10.1007/s10584-010-9834-5
3. Coles, S. (2001). An Introduction to Statistical Modeling of Extreme Values. Springer. https://doi.org/10.1007/978-1-4471-3675-0
4. Fisher, R. A. (1934). The effect of methods of ascertainment upon the estimation of frequencies. Annals of Eugenics, 6(1), 13-25. https://doi.org/10.1111/j.1469-1809.1934.tb02105.x
5. Rao, C. R. (1965). On discrete distributions arising out of methods of ascertainment. Sankhyā: The Indian Journal of Statistics, Series A, 27(4), 311-324. https://doi.org/10.1007/978-1-4612-0913-3_13
6. Ghil, M. (2011). Nonlinear and nonstationary climate dynamics. Wiley Interdisciplinary Reviews: Climate Change, 2(6), 805-827. https://doi.org/10.1002/wcc.138
7. Alzaatreh, A., Lee, C., & Famoye, F. (2013). A new method for generating families of continuous distributions. Metron, 71(1), 63-79. https://doi.org/10.1007/s40300-013-0007-y
8. Carrasco, J. M. F., Ortega, E. M. M., & Cordeiro, G. M. (2008). A generalized modified Weibull distribution for lifetime modeling. Computational Statistics & Data Analysis, 53(2), 450-462. https://doi.org/10.1016/j.csda.2008.08.023
9. Patil, G. P., & Rao, C. R. (1978). Weighted distributions and size-biased sampling with applications to wildlife populations and human families. Biometrics, 34(2), 179-189. https://doi.org/10.2307/2530008

10. Seneviratne, S. I., et al. (2012). Changes in climate extremes and their impacts on the natural physical environment. In Managing the Risks of Extreme Events and Disasters to Advance Climate Change Adaptation. Cambridge University Press. https://doi.org/10.1017/CBO9781139177245.006
11. Mahdavi, A., & Kundu, D. (2017). Weighted Weibull distribution: Theory and applications. Communications in Statistics - Theory and Methods, 46(2), 767-783. https://doi.org/10.1080/03610926.2015.1006777
12. Press, W. H., Teukolsky, S. A., Vetterling, W. T., & Flannery, B. P. (2016). Numerical Recipes: The Art of Scientific Computing (3rd ed.). Cambridge University Press. https://doi.org/10.2307/3616529
13. Mishra, A. K., & Singh, V. P. (2010). A review of drought concepts. Journal of Hydrology, 391(1-2), 202-216. https://doi.org/10.1016/j.jhydrol.2010.07.012
14. Hosking, J. R. M. (1990). L-moments: Analysis and estimation of distributions using linear combinations of order statistics. Journal of the Royal Statistical Society: Series B, 52(1), 105-124. https://doi.org/10.1111/j.2517-6161.1990.tb01775.x
15. Zscheischler, J., et al. (2018). Future climate risk from compound events. Nature Climate Change, 8(6), 469-477. https://doi.org/10.1038/s41558-018-0156-3
16. Arnold, B. C., & Sarabia, J. M. (2015). Majorization and the Lorenz Order with Applications in Applied Mathematics and Economics. Springer. https://doi.org/10.1007/978-3-319-13930-4
17. Westfall, P. H. (2014). Kurtosis as peakedness, 1905-2014. The American Statistician, 68(3), 191-195. https://doi.org/10.1080/00031305.2014.917055
18. Guess, F. M., & Proschan, F. (1988). Mean residual life: Theory and applications. In Handbook of Statistics (Vol. 7, pp. 215-224). Elsevier. https://doi.org/10.1016/S0169-7161(88)07013-3
19. Anderson, T. W. (2010). Reliability and survival analysis. In International Encyclopedia of Statistical Science (pp. 1191-1194). Springer. https://doi.org/10.1007/978-3-642-04898-2_483
20. Rényi, A. (1961). On measures of entropy and information. In Proceedings of the Fourth Berkeley Symposium on Mathematical Statistics and Probability (Vol. 1, pp. 547-561). University of California Press. https://doi.org/10.1525/9780520375713-027
21. Cover, T. M., & Thomas, J. A. (2012). Elements of Information Theory (2nd ed.). Wiley. https://doi.org/10.1002/0471748824
22. Kleiber, C., & Kotz, S. (2003). Statistical Size Distributions in Economics and Actuarial Sciences. Wiley. https://doi.org/10.1002/0471457175
23. Casella, G., & Berger, R. L. (2024). Statistical Inference (2nd ed.). Chapman and Hall/CRC. https://doi.org/10.1201/9781003456285
24. R Core Team. (2023). R: A Language and Environment for Statistical Computing. R Foundation for Statistical Computing. https://doi.org/10.32614/RJ-2023-001
25. Donat, M. G., et al. (2016). Updated analyses of temperature and precipitation extreme indices since the beginning of the twentieth century. Journal of Geophysical Research: Atmospheres, 121(10), 5730-5752. https://doi.org/10.1002/2015JD024045
26. Marsaglia, G., Tsang, W. W., & Wang, J. (2003). Evaluating Kolmogorov's distribution. Journal of Statistical Software, 8(18), 1-4. https://doi.org/10.18637/jss.v008.i18
27. Akaike, H. (1998). Information theory and an extension of the maximum likelihood principle. In Selected Papers of Hirotugu Akaike (pp. 199-213). Springer. https://doi.org/10.1007/978-1-4612-1694-0_15
28. Perkins, S. E., Alexander, L. V., & Nairn, J. R. (2012). Increasing frequency, intensity and duration of observed global heatwaves. Geophysical Research Letters, 39(20), L20714. https://doi.org/10.1029/2012GL053361
29. Sillmann, J., et al. (2013). Climate extremes indices in the CMIP5 multimodel ensemble. Journal of Geophysical Research: Atmospheres, 118(4), 1716-1727. https://doi.org/10.1002/jgrd.50203

30. IPCC. (2022). Climate Change 2022: Impacts, Adaptation and Vulnerability. Contribution of Working Group II to the Sixth Assessment Report of the Intergovernmental Panel on Climate Change. Cambridge University Press. https://doi.org/10.1017/9781009325844
31. Zscheischler, J., et al. (2020). A typology of compound weather and climate events. Nature Reviews Earth & Environment, 1(7), 333-347. https://doi.org/10.1038/s43017-020-0060-z
32. Gelman, A., et al. (2013). Bayesian Data Analysis (3rd ed.). Chapman and Hall/CRC. https://doi.org/10.1201/b16018
33. Kingsley, E. S., & Badmus, N. I. (2025). Assessing the efficiency of maximum likelihood, interquartile range, and Monte Carlo methods for estimating Weibull distribution parameters. Annals of Mathematics and Computer Science, 26, 1–15. https://doi.org/10.56947/amcs.v26.449
34. Dabye, A. S., Diakhate, D., & Fall, M. M. Markov and Hidden Markov Models for genomic sequence classification. Annals of Mathematics and Computer Science, 35. https://doi.org/10.56947/amcs.v35.852

[1] Department of Mathematics, Kisii University, P.O. Box 408-40200, Kisii, Kenya.

Email address: fmonari@kisiiuniversity.ac.ke